



Interactive Segmentation Technique for Ex-Vivo Skin Laceration Detection

Varnita Verma¹, Anil Kumar², Piyush Chauhan³ and Mukul Kumar Gupta⁴

¹Doctoral Research Fellow, Department of Electrical and Electronics Engineering, University of Petroleum and Energy Studies, Dehradun (Uttarakhand), India.

²Assistant Professor, Department of Computer Science, University of Petroleum and Energy Studies, Dehradun (Uttarakhand), India.

³Assistant Professor, Department of Computer Science, University of Petroleum and Energy Studies, Dehradun (Uttarakhand), India.

⁴Assistant Professor, Department of Electrical and Electronics Engineering, University of Petroleum and Energy Studies, Dehradun (Uttarakhand), India.

(Corresponding author: Varnita Verma)

(Received 29 February 2020, Revised 23 April 2020, Accepted 25 April 2020)

(Published by Research Trend, Website: www.researchtrend.net)

ABSTRACT: In the current scenario, the working culture in industries are improving day by day in terms of human safety and increase in awareness regarding safeguard required for performing different operations. Still while performing the task in industries, home or doing normal routine work the skin laceration is very common. For laceration detection and localization on the patient, the doctor should identify the edges of laceration specifically so that during the tissue approximation for in-vivo or ex-vivo operation the localization maneuverer robot region of interest can be identified. The major issue faced during skin laceration segmentation is identification of lesion edges. The existing algorithms marked issues like poor skin segmentation, altered result with respect to ambient light, inability for laceration segmentation in the complex background image and less noise rejection while identifying the laceration. In this paper, the interactive skin laceration segmentation technique with hybrid sequential approach is used to overcome the limitations in existing algorithms to detect the skin laceration. The proposed hybrid sequential approach for interactive selection of skin laceration segmentation used HSV based color segmentation along with Euclidean distance metric and Geodesic distance metric. The results were compared for the performance of the best hybrid sequential combination.

Keywords: Euclidean distance Metric, Geodesic distance Metric, HSV Colour Space, Interactive Image Processing, Marking Based Segmentation Technique (MBST), Medical Imaging, Skin laceration detection, Skin Phantom.

I. INTRODUCTION

This skin segmentation is one of the most studies and fundamental problems in biomedical imaging. The common difficulty faced by the researcher is to identify the skin segmentation as the skin texture varies from person to person. This produced the ambiguous results for a set parameter threshold values. Interactive segmentation techniques have been used before to trace the part of desired object from its background [1-3]. In skin segmentation technique, the researchers frequently used bounding box as an identifier around the desired object [4]. The ultimate goal of researcher is to segment the desired object from its background with minimal efforts [5-7].

We focus on the technique where the researcher marks on the object of interest with respect to the background in order to seed segmentation known as marking based segmentation technique (MBST) [8, 9]. This approach requires less accurate input provided by the researcher to estimate the required region of interest (ROI). The bounding box based segmentation technique (BBST) for segmentation allows the researcher to draw a bounding box over the ROI [4, 10]. BBST approach is simpler but has less control over the output parameters whereas MBST results are relatively having more control and refined results.

The marking based segmentation technique has been used by many researchers explicitly or conceptually [11-

13]. MBST technique works outwards to the marked segment to attain the desired ROI. This method is useful to select the desired complex boundaries ROI. Thin and long objects are considered to be complex boundary objects because it is difficult for the researcher to mark the desired object pixels. This article illustrates the new method of interactive segmentation in which the researcher can mark the pixel of the desired object also termed as seeding to segment the image. The Euclidean distance Metric and Geodesic distance metric were the two different MBST techniques that were implemented and compared in this article. Before implementing a segmentation algorithm some color based preprocessing is required on the test image to achieve an indistinct color model irrespective of ambient lighting condition [14]. This entire system is developed to segment ex-vivo skin laceration termed as the Skin Laceration Detection System.

II. REVIEW OF IMAGE SEGMENTATION IN MEDICAL DIAGNOSIS

In medical diagnosis the medical image segmentation is frequently used in various domains of medical research such as Microbiology, Pathology, Preoperative planning of different Surgeries, Radiology, Dermatology, etc [15]. The popular image segmentation use to analyze the health condition of patients are X-Rays, CT scan, MRI, etc. In Dermatology, a large amount of skin

segmentation is required to detect minor cases like allergy, pimples to extreme cases like cancer and eczema. The skin lesion detection is the basic requirement for complex surgeries. Ex-vivo skin laceration detection the first step before any surgery. To detect the boundary of laceration the different segmentation techniques were used by the researchers such as K-means algorithm, Graph cut [8, 16], multiple thresholding [7, 17], adaptive GMMRF [18], Euclidean distance metric [19, 20], Geodesic distance metric algorithm [8, 21], etc. The boundary of skin lesion may vary with inner surface. The results of ex-vivo skin lesion segmentation may vary with varying luminescence [6, 14]. The previously discussed studies involves predictive methods which is more susceptible to falls estimation of laceration. The proposed method is cost effective and interactive method, which enables surgeon to locate Region of Interest (ROI).

III. SKIN LACERATION DETECTION TECHNIQUE

The laceration detection algorithm includes four major steps that include image acquisition, image preprocessing, feature extraction and recognition. The skin phantom is used to detect the laceration using proposed MBST. The test image for laceration detection can be seen in Fig. 1.



Fig. 1. Skin Phantom.

A. Image Acquisition

The test image can be captured in two ways: Real-Time and manual mode. In Real-Time Mode the test image will be captured using a digital camera and simultaneously the test image will pass on to further steps. In manual mode, the pre-existing image from storage in jpg format is feed to the system algorithm.

B. Image Pre-processing

In this step, the essential modulation in the captured test image is done to feed the required correct information to the system algorithm. This includes resizing, Colour space correction, etc. of the test image. Resizing of test image is used to maintain the uniformity in the size of input test image. The colour space correction includes conversion of Input RGB image into other colour spaces such as Grey Colour space, HSV Colour space, etc. [7, 22-25]. In this proposed laceration detection algorithm, the RGB Colour Space has converted into HSV Colour Space. HSV includes two channels in which H represents the chrominance channel, S represents colour and luminance channel whereas V represents the texture feature of an input image. The following are the equations of colour space conversion from RGB to HSV.

$$H = \cos^{-1} \left\{ \frac{0.5[(R - G) + (R - B)]}{\left[\frac{(R - G)^2 + (R - B)(G - B)}{3} \right]^{0.5}} \right\} \quad (1)$$

$$S = 1 - \frac{\min(R + G + B)}{3} \quad (2)$$

$$V = \frac{1}{3}(R + G + B) \quad (3)$$

HSV colour space is robust to varying camera direction and illuminance. Fig. 2 represents the HSV Converted test image.



Fig. 2. HSV Image of Skin Phantom.

C. Feature Extraction

Feature extraction plays a major role in image segmentation. There is n number of ways to extract the desired features from the image. The 8 color features and 5 texture features were extracted from the HSV color space of the desired object. The HSV color features include mean, standard deviation, skewness, Kurtosis and so on. In texture features include energy, entropy, contrast, correlation, Homogeneity [19, 26]. In the proposed laceration detection system, the interactive selection of the color space of ROI is given by the researcher. As per the interactive selection made by the researcher the above-mentioned color and texture feature from converted HSV image is stored as a featured database which is therefore used as the desired feature by the algorithm. Figure 3 represents the desired feature of a skin laceration detection system. Similarly, the test image features were computed by the feature extraction technique.

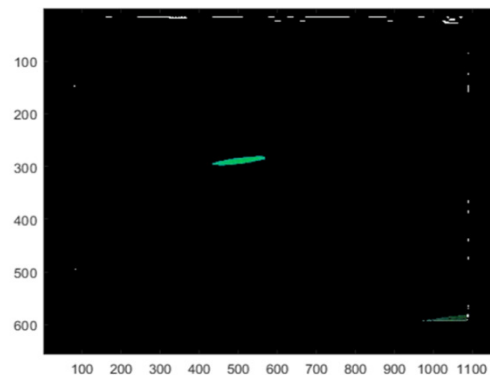


Fig. 3. Interactive selection of desired HSV color space.

Then the test image features were compared with the featured database of ROI through two different algorithms such as Euclidean Distance metric and Geodesic distance metric.

D. Geodesic Segmentation

Geodesic segmentation is robust enough to segment thin and long structures irrespective of its boundary length. The formulation of the Geodesic distance metric for the unary region term is given as in Eqn. 4. $M_l(x_i)$ represents the global colour model, $G_l(x_i)$ is geodesic distance formulated by using the related desired object/background geodesic distance with respect researcher input marker as stated in Eqn. 5.

$$R_l(x_i) = s_l(x_i) + M_l(x_i) + G_l(x_i) \quad (4)$$

$$G_l(x_i) = \frac{D_l(x_i)}{D_F(x_i) + D_B(x_i)} \quad (5)$$

Where ∂_l represents the set of seeds with label $l \in \{F\}$. In this method, the conjugate \bar{l} is considered as the set of seeds with the label $\bar{l} \in \{B\}$.

$$s_l(x_i) = \begin{cases} \infty & \text{if } x_i \in \partial_l \\ 0 & \text{otherwise} \end{cases} \quad (6)$$

With the help of Fast Gauss Transform the desired object/background colour model $P_l(C)$ was computed and stated in Eqn. 7.

$$M_l(x_i) = P_l(C(x_i)) \quad (7)$$

The computed boundary term can be stated as in Eqn. 8.

$$B(x_0, x_1) = \frac{1}{1 + \|C(x_i) - C(x_j)\|^2} \quad (8)$$

Where, $C(x) \in [0,255]$.

E. Euclidean Distance Segmentation

Euclidean distance segmentation requires the accurate distance of pixels to achieve precise results. Metric coefficient defines Euclidean distance which depends on pixel information. Euclidean distance has insensitivity towards the minor deformations. Let $P_i P_j$ are the pixels

of image where $ij = 1,2,3,\dots,MN$. The e_i represents the coordinate system of image space. The metric coefficient g_{ij} of image can be determined by Eqn. 9.

$$g_{ij} = \langle e_i, e_j \rangle = \sqrt{\langle e_i, e_i \rangle} \sqrt{\langle e_j, e_j \rangle} \cos \theta_{ij} \quad (9)$$

where \langle, \rangle represents scalar product, θ_{ij} is the angle between e_i and e_j . When base vectors are of same length then g_{ij} totally depends upon θ_{ij} . Then the Euclidean distance of two image spaces x, y will be computed as stated in Eqn. 10.

$$d_E^2(x, y) = \sum_{i,j=1}^{MN} g_{ij} (x^i - y^i)(x^j - y^j) = (x - y)^T G (x - y) \quad (10)$$

The Euclidean distance segmentation is robust and more accurate segmentation technique for medical imaging where the results depends upon the Euclidean distance computation. The segmented image pixels and number of pixels retained in rows and columns where stored. The total number of pixel in image can be written as stated below in Eqn. 11.

$$p = R * C \quad (11)$$

Where p represents Total number of Pixels which is equivalent to product of pixels in Rows (R) and Number of pixels in Columns (C) of image.

Fig. 4 represents the flow chart for the skin laceration detection system, which provides information about the steps required to be followed for the detection of skin laceration. The process of conversion of test image into desired segmented image as discussed above is pictorially represented in flow chart for easy understanding of algorithm for researchers. The performance of algorithm is evaluated on the bases of number of information pixels.

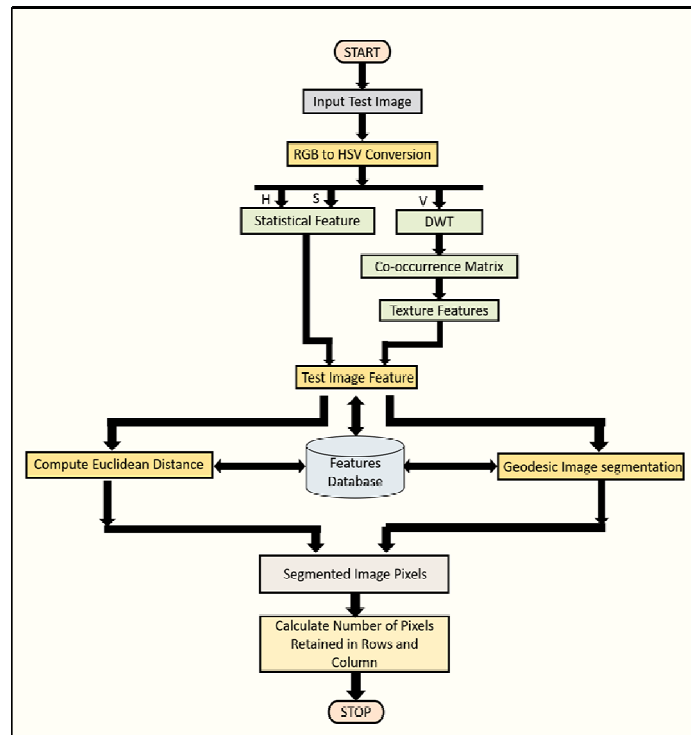


Fig. 4. Flow chart for Skin laceration detection system.

IV. RESULTS

The Skin laceration detection system was provided with the skin phantom test image. The results of Euclidean distance metric algorithm with varying tolerance is shown in Fig. 5. The detected ROI of skin laceration can be seen with highlighted blue colour grown region. The 0.2 tolerance value of the Euclidean distance metric algorithm shows poor results as compared with 0.05, 0.1 and 0.15 tolerance results. Similarly, the results of the Geodesic distance metric algorithm with varying tolerance is shown in Fig. 6.

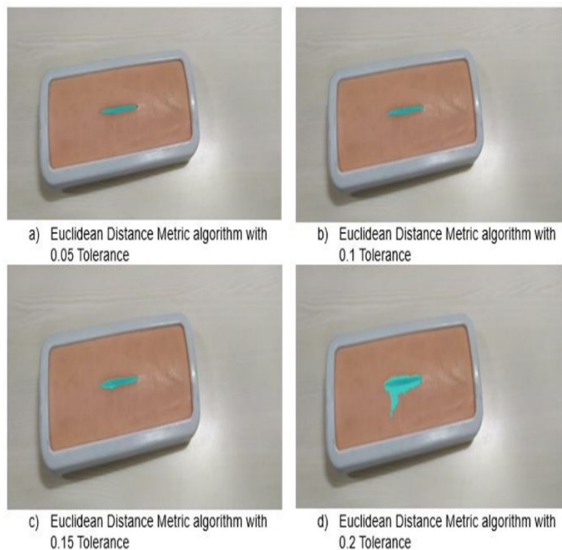


Fig. 5. Laceration segmentation of Phantom using Euclidean Distance Metric algorithm with varying Tolerance.

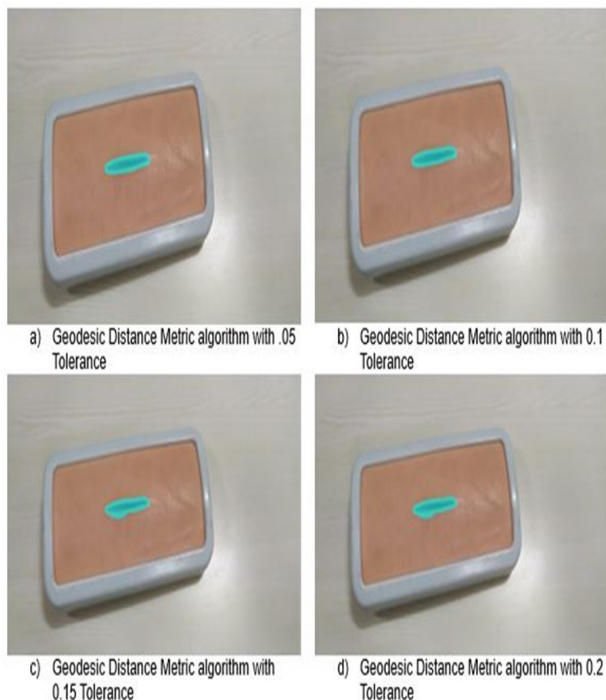


Fig. 6. Laceration segmentation of Phantom using Geodesic Distance Metric algorithm with varying Tolerance.

The 0.2 tolerance value of the Geodesic distance metric algorithm shows poor results as compared with 0.05, 0.1 and 0.15 tolerance results. The best skin laceration segmentation results can be seen using Euclidean distance metric algorithm with 0.05 tolerance value. The number of pixels of the segmented ROI provides an accurate measure for the efficiency of the algorithm. Total pixel of an image can compute as the multiplication of number of pixels in rows to number of pixels in columns.

Efficiency calibration of the algorithm can be computed with the help of information pixels. On applying different tolerance to the segmentation algorithms the number of pixels representing in rows and columns of the segmented ROI can be seen in Table 1.

Table 1: Comparison table for Euclidean distance metric with respect to Geodesic Distance Metric.

Distance Metric	Tolerance	Rows	column
Euclidean	0.05	1047	1648
Euclidean	0.1	1059	1679
Euclidean	0.15	1051	1660
Euclidean	0.2	1047	1671
Geodesic	0.05	1051	1660
Geodesic	0.1	1043	1644
Geodesic	0.15	1051	1652
Geodesic	0.2	1043	1664

The total number of pixels representing the ROI of the skin laceration on applying different algorithms Euclidean and Geodesic distance metric concerning varying tolerance were projected using Fig. 7. The segmented ROI of skin laceration with its pixels can be seen in Fig. 8.

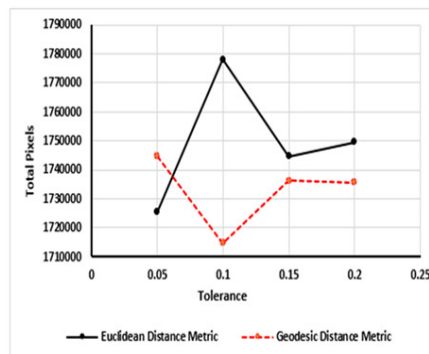


Fig. 7. Comparative analysis of Total pixels required for each Euclidean and Geodesic Distance metric algorithm for laceration detection.

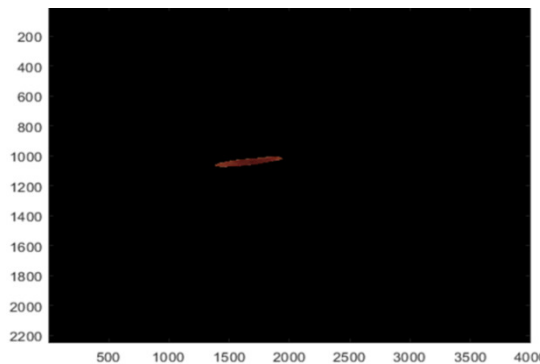


Fig. 8. Segmentation of Skin laceration.

V. CONCLUSION

The effective, efficient and interactive skin laceration image segmentation algorithm is illustrated in this paper. This paper illustrates the proposed skin laceration detection system. The Euclidean distance segmentation algorithm and Geodesic segmentation algorithm were implemented on our test skin Phantom image. The results of both algorithms are compared with each other with varying tolerance. The experiment results show that Euclidean distance Segmentation produced good results as compared to Geodesic Segmentation. This advanced imaging technique will help in more accurate and robust skin laceration assessment. The measurement of area and volume of laceration helps surgeon to estimate suture points.

VI. FUTURE SCOPE

Current research has a potential to offer inputs for those interested in detecting the skin laceration. This research can be used as the pre-operative stage for wound closure technique. The predictive estimation of wound healing parameters and various disease associated can be identified.

ACKNOWLEDGMENT

The authors wish to thank the Center of Excellence at the University of Petroleum and Energy Studies for logistic support. This work was supported in part by a seed grant from the Research and Development Department of the University of Petroleum and Energy Studies.

Conflict of Interest. The authors confirm that there are no known conflicts of interest associated with this publication of this paper.

REFERENCES

[1]. Olabarriga, S. D., & Smeulders, A. W. M. (2001). Interaction in the segmentation of medical images: A survey. *Medical Image Analysis*, 5, 127–142.

[2]. Peng, Z., Shj, Q., Qu, S., & Li, Q. (2019). Interactive image segmentation using geodesic appearance overlap graph cut Interactive image segmentation using geodesic appearance overlap graph cut ☆. *Signal Processing: Image Communication*, 78, 159–170.

[3]. Protiere, A., & Sapiro, G. (2007). Interactive image segmentation via adaptive weighted distances. *IEEE Transactions on Image Processing*, 16(4), 1046–1057.

[4]. bin Abdul Rahman, N. A., Wei, K. C., & See, J. (2006). RGB-H-CbCr Skin Colour Model for Human Face Detection. *Proceedings of the MMU International Symposium on Information & Communications Technologies (M2USIC 2006)*, 90–96.

[5]. Abdullah-Al-Wadud, M., & Chae, O. (2008). Region-of-Interest Selection for Skin Detection Based Applications. In *International Conference on Convergence Information Technology*, 1999–2004. Institute of Electrical and Electronics Engineers (IEEE).

[6]. Kolkur, S., Kalbande, D., Shimpi, P., Bapat, C., & Jatakia, J. (2017). Human Skin Detection Using RGB, HSV and YCbCr Color Models. In *International Conference on Communication and Signal Processing*, 137, 324–332.

[7]. Gasparini, F., & Schettini, R. (2006). Skin segmentation using multiple thresholding. *Internet Imaging VII*, 6061(60610), 60610F.

[8]. Price, B. L., Morse, B., & Cohen, S. (2010). Geodesic graph cut for interactive image segmentation. In *Proceedings of the IEEE Computer Society Conference on Computer Vision and Pattern Recognition*, 3161–3168.

[9]. Marcel, S., Bernier, O., Viallet, J. E., & Collobert, D. (2000). Hand gesture recognition using input-output hidden markov models. In *Proceedings Fourth IEEE International Conference on Automatic Face and Gesture Recognition (Cat. No. PR00580)*, 456–461.

[10]. Verma, V., Rajput, A., Chauhan, P., Rathore, H., Goyal, P., & Gupta, M. K. (2019). 7 Machine vision for human-machine interaction using hand gesture recognition. In *Intelligent Decision Support Systems*, 155–181.

[11]. Rother, C., Kolmogorov, V., & Blake, A. (2004). “GrabCut” - Interactive foreground extraction using iterated graph cuts. In *ACM Transactions on Graphics*, 23, 309–314.

[12]. Fard, M. J., Ameri, S., Chinnam, R. B., & Ellis, R. D. (2016). Soft Boundary Approach for Unsupervised Gesture Segmentation in Robotic-Assisted Surgery. *Robotics and Automation Letters*, 2(1), 171–178.

[13]. Kumar, K. S., Jacob, C. F., & Reddy, B. E. (2014). Unsupervised wound image segmentation. *ICTACT Journal on Image & Video Processing*, 4(3), 737–747.

[14]. Ueng, S. K., & Chang, C. Y. (2016). Skin color model adaptation under varying lighting conditions. *Advances in Mechanical Engineering*, 8(9), 1–8.

[15]. Verma, V., Chowdary, V., Gupta, M. K., Mondal, A. K., Chowdary, V., Gupta, M. K., & Mondal, A. K. (2018). IoT and Robotics in Healthcare. In *Medical Big Data and Internet of Medical Things*, 245–269. Boca Raton: Taylor & Francis, [2019]: CRC.

[16]. Lombaert, H., Sun, Y., L. G. (2005). A multilevel banded graph cuts method for fast image segmentation. In *Tenth IEEE International Conference on Computer Vision (ICCV'05)*, 259–265.

[17]. Sankaran, S., Hagerty, J. R., Malarvel, M., Sethumadhavan, G., & Stoecker, W. V. (2019). A comparative assessment of segmentations on skin lesion through various entropy and six sigma thresholds. In *Lecture Notes in Computational Vision and Biomechanics*, 30, 179–188.

[18]. Blake, A., Rother, C., Brown, M., Perez, P., & Torr, P. (2004). Interactive image segmentation using an adaptive GMMRF model. In *European conference on computer vision*, 428–441.

[19]. Selvarasu, N., Nachiappan, A., & Nandhitha, N. M. (2010). Abnormality detection from medical thermographs in human using Euclidean distance based color image segmentation. In *2010 International Conference on Signal Acquisition and Processing, ICSAP 2010*, 73–75.

[20]. Canalini, L., Klein, J., Miller, D., & Kikinis, R. (2019). Registration of ultrasound volumes based on euclidean distance transform. In *Lecture Notes in Computer Science (including subseries Lecture Notes in Artificial Intelligence and Lecture Notes in Bioinformatics)*, 127–135).

- [21]. Niessen, W. J., Romeny, B. M. T. H., & Viergever, M. A. (1998). Geodesic deformable models for medical image analysis. *IEEE Transactions on Medical Imaging*, 17(4), 634-641.
- [22]. Ibraheem, N. A., Khan, R. Z., & Hasan, M. M. (2013). Comparative study of skin color based segmentation techniques. *International Journal of Applied Information Systems*, 5(10), 24-39.
- [23]. Jena, K. K., Mishra, S., Mishra, S., & Bhoi, S. K. (2019). An Edge based Steganographic Approach using a two Level Security Scheme for Digital Image Processing and Analysis. *International Journal on Emerging Technologies*, 10(2), 29-38.
- [24]. Patel, H., & Deshpande, A. (2019). Reliability Evaluation of Renewable Energy Integrated Power System in Presence of Energy Storage System. *International Journal on Emerging Technologies*, 10(4), 380-384.
- [25]. Mishra, A. K., Singh, J., & Tiwari K. N. (2019). In Vitro Regeneration of Clitoria ternatea (L.) from Nodal Explant. *International Journal on Emerging Technologies*, 10(1), 35-41.
- [26]. Reddy, P. S., Soni, H., & Afroze, M. S. (2013). DA DWT-IDWT based Image Compression Implementation. *International Journal of Electrical, Electronics and Computer Engineering* 2(2): 113-116.
- Reddy, P. S., Soni, H., & Afroze, M. S. DA DWT-IDWT based Image Compression Implementation.
- [27]. Lucas, Y., Niri, R., Treuillet, S., Douzi, H., & CASTANEDA, B. A. (2020). Wound Size Imaging: Ready for Smart Assessment and Monitoring. *Advances in Wound Care*, (ja).

How to cite this article: Verma, V., Kumar, A., Chauhan, P. and Gupta, M. K. (2020). Interactive Segmentation Technique for Ex-Vivo Skin Laceration Detection. *International Journal on Emerging Technologies*, 11(3): 371-376.